Neighbor GRPO: Contrastive ODE Policy Optimization Aligns Flow Models

Dailan He^{1,2} Guanlin Feng² Xingtong Ge^{2,3} Yazhe Niu¹ Yi Zhang² Bingqi Ma² Guanglu Song² Yu Liu² Hongsheng Li^{1,4,5}

¹CUHK MMLab ²Vivix.AI ³HKUST ⁴Shenzhen Loop Area Institute ⁵CPII under InnoHK

Abstract

Group Relative Policy Optimization (GRPO) has shown promise in aligning image and video generative models with human preferences. However, applying it to modern flow matching models is challenging because of its deterministic sampling paradigm. Current methods address this issue by converting Ordinary Differential Equations (ODEs) to Stochastic Differential Equations (SDEs), which introduce stochasticity. However, this SDE-based GRPO suffers from issues of inefficient credit assignment and incompatibility with high-order solvers for fewer-step sampling. In this paper, we first reinterpret existing SDE-based GRPO methods from a distance optimization perspective, revealing their underlying mechanism as a form of contrastive learning. Based on this insight, we propose Neighbor GRPO, a novel alignment algorithm that completely bypasses the need for SDEs. Neighbor GRPO generates a diverse set of candidate trajectories by perturbing the initial noise conditions of the ODE and optimizes the model using a softmax distance-based surrogate leaping policy. We establish a theoretical connection between this distance-based objective and policy gradient optimization, rigorously integrating our approach into the GRPO framework. Our method fully preserves the advantages of deterministic ODE sampling, including efficiency and compatibility with highorder solvers. We further introduce symmetric anchor sampling for computational efficiency and group-wise quasinorm reweighting to address reward flattening. Extensive experiments demonstrate that Neighbor GRPO significantly outperforms SDE-based counterparts in terms of training cost, convergence speed, and generation quality.

1. Introduction

Building on the success of Reinforcement Learning from Human Feedback (RLHF) [2, 23, 32] and Reinforcement Learning with Verifiable Rewards (RLVR) [5, 13] in text generation, the application of Reinforcement Learning (RL) to align visual generative models with human preference is now a burgeoning field of research. Among

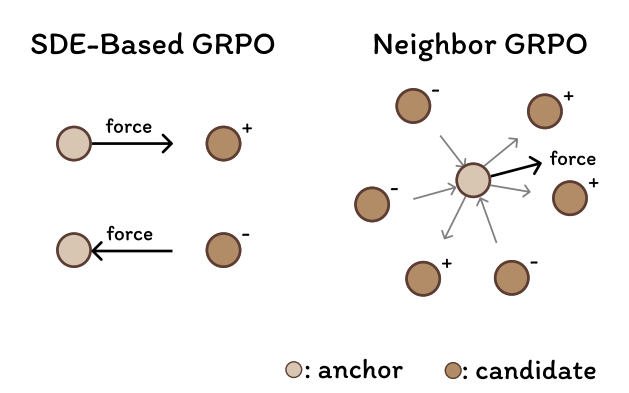


Figure 1. GRPO approaches for flow models optimize the sample x_t at each timestep t. We revisit it from the perspective of contrastive learning, pushing anchor samples to high-reward candidates and vice versa. Different from SDE-based GRPO approaches [17, 41] that conduct sample-wise exploration and optimization, our Neighbor GRPO optimizes the policy at the anchor in a joint force field defined by all candidates in a group. This approach allows full-ODE training, leading to better training efficiency and sample quality.

the various techniques, Group Relative Policy Optimization (GRPO) [29] stands out as a powerful policy gradient method. By eliminating the need for an expensive critic network, GRPO achieves stable and efficient policy optimization, even with simple reward functions or rule-based verifiers. Specifically, the adaptation of GRPO to text-to-image diffusion models [7, 21, 24, 30, 43] and flow matching models [12, 16] has yielded promising results [14, 15, 17, 36, 41], with these methods showing superior performance in human preference alignment. Unlike previous alignment approaches [3, 33, 35, 39, 40], those GRPO methods present stronger flexibility, requiring neither differentiable reward models nor paired human preference annotations.

State-of-the-art text-to-image generation models such as FLUX [12] have adopted a generation paradigm based on flow matching [16], which learns deterministic Ordinary Differential Equation (ODE) trajectories, defining fromnoise-to-data probability flows. However, applying GRPO to flow matching models introduces a fundamental conflict:

GRPO relies on stochasticity to explore the policy space, whereas the core advantage of flow matching models lies in their efficient, high-quality deterministic sampling. Existing approaches, such as Flow-GRPO [17] and Dance-GRPO [41], primarily address this conflict by employing Stochastic Differential Equations (SDEs). This SDE-based GRPO approach converts the deterministic ODE into an equivalent SDE, modeling the reverse denoising process as a Markov decision process (MDP). This enables policy gradient-based RLHF optimization methods like GRPO.

However, this conversion sacrifices the core advantages of ODEs. Firstly, SDE sampling is often restricted to first-order solvers, making it difficult to leverage more efficient high-order solvers like DPM-Solver++ [20]. Secondly, SDE training is relatively inefficient due to the mismatch in credit assignment between reward scores and single-step noise injection [15]. Subsequent works like MixGRPO [14] and BranchGRPO [15] have partially mitigated the computational efficiency issues through techniques like mixed sampling and branch reuse, but they remain constrained by the inherent limitations of the SDE framework and face the challenge of credit assignment, *i.e.* the terminal reward signal must be distributed across all timesteps. Hence, a novel paradigm is urgently needed.

We re-examine the optimization mechanism of GRPObased flow matching from the perspective of inter-sample distance optimization. For existing SDE-based GRPO schemes, at each sampling step, we can reinterpret the optimization dynamics: if we consider the deterministically computed sample from the ODE as an anchor and the stochastically sampled counterparts from the SDE as candidates, optimizing the SDE policy gradient is equivalent to pulling the anchor closer to high-reward candidates while pushing it away from low-reward ones. This dynamic is illustrated in Figure 1. Therefore, the SDE-based GRPO optimization process can be understood as a form of contrastive learning [1, 4, 6, 25] based on the distance between the anchor and candidate samples. Since the candidate samples obtained from SDE sampling are random perturbations of the ODE anchor, this contrastive learning process guides the model to explore positive and negative samples in the neighborhood and determine the optimization direction.

From this perspective, we propose a more direct approach: we generate a set of candidate trajectories by perturbing the initial conditions of the ODE, effectively creating a neighborhood around the original ODE path. We then select one trajectory as the anchor and the others as candidates, applying a distance-based loss to pull the anchor towards high-reward candidates and push it away from low-reward ones. Inspired by contrastive learning, we adopt an advantage-guided soft nearest-neighbor optimization to achieve this distance optimization. The key finding is that the softmax distribution corresponding to this objective de-

fines a surrogate leaping policy in the ODE neighborhood. This policy introduces the necessary stochasticity for exploring the deterministic ODE process by performing single-step random transitions on neighborhood samples according to the softmax distribution of anchor-candidate distances. Based on this surrogate policy, we can rigorously integrate distance optimization directly into the GRPO framework, allowing the entire optimization process to break free from its dependence on SDE sampling and achieve effective reinforcement learning while fully preserving all the advantages of ODEs. We further investigate key points for practical implementation: (1) a symmetric anchor sampling strategy to accelerate policy updates; (2) the direct use of high-order solvers like DPM++ [20]; and (3) a quasinorm reweighting mechanism to address reward hacking by sharpening the often-flat GRPO advantage vector. Both qualitative and quantitative results demonstrate that our proposed approach outperforms existing methods in text-toimage generation with only 4 hours of training.

In this paper, we propose Neighbor GRPO, a novel RLHF method for flow matching models. Our main contributions include:

- 1. We reinterpret GRPO in flow matching from a distance optimization perspective, revealing its connection to contrastive learning.
- We propose Neighbor GRPO based on a discrete surrogate policy, which constructs a contrastive learning objective in the ODE neighborhood. This achieves effective policy optimization while fully preserving the advantages of ODE solvers.
- 3. We demonstrate that Neighbor GRPO can outperform existing SDE-based methods in terms of training cost and generation quality through extensive experiments.

2. Related Works

The application of RLHF to visual generative models has evolved rapidly, with GRPO [29] emerging as a particularly effective approach due to its stability and elimination of expensive critic networks. We categorize recent advances into two waves: pioneering GRPO adaptations designed for flow models and efficiency improvements for practice.

Flow-GRPO [17] and DanceGRPO [41] successfully integrate online RL with flow matching models by converting the deterministic ODE into an equivalent SDE, enabling stochastic exploration while maintaining marginal probability distributions. DanceGRPO extends this approach to a broader range of visual generation tasks (text-to-image, text-to-video, image-to-video) and emphasizes key implementation details such as shared noise initialization to prevent reward hacking. MixGRPO [14] introduces a hybrid ODE-SDE sampling strategy with a sliding window mechanism. By restricting SDE sampling and GRPO optimization to a window that slides from high-noise to low-noise re-

gions, it significantly reduces training costs while achieving better performance. BranchGRPO [15] tackles efficiency and credit assignment from a different angle by replacing independent sequential rollouts with a branching tree.

Our work builds upon these advances but takes a fundamentally different approach. While existing methods rely on SDE conversion, we propose a novel perspective that reinterprets SDE-based GRPO as distance-based contrastive learning and introduces a surrogate leaping policy that enables effective RLHF while preserving all the advantages of deterministic ODE sampling.

3. Methodology

In this section, we present Neighbor GRPO, a novel RLHF method for flow matching models that bypasses the need for SDE conversion. We begin by establishing necessary background on flow matching and SDE-based GRPO methods (Section 3.1). We then reinterpret existing SDE-based GRPO approaches from the perspective of distance-based contrastive learning (Section 3.2). Building on this insight, we introduce Neighbor GRPO (Section 3.3), which constructs a neighborhood of candidate trajectories by perturbing initial noise conditions and defines a softmax distance-based surrogate leaping policy to enable policy gradient optimization while preserving deterministic ODE sampling. Finally, we present three key implementation strategies of our proposed Neighbor GRPO (Section 3.4).

3.1. Preliminary

Flow Matching Models. Flow matching models [16] generate samples by learning deterministic Ordinary Differential Equation (ODE) trajectories from noise to data. Its forward and backward processes are defined as

$$x_t = (1 - t)x + t\epsilon, \quad t \in [0, 1],$$
 (1)

$$x_{t-\Delta t}^{(\text{ODE})} = x_t - \Delta t v_{\theta}(x_t, t), \quad \Delta t > 0,$$
 (2)

where x is a data sample and $\epsilon \sim \mathcal{N}(0,I)$ is standard Gaussian noise. The model learns a velocity field $v_{\theta}(x_t,t)$ such that the reverse denoising process can be solved similarly to v-prediction diffusion models. This deterministic property gives flow matching a significant advantage in sampling efficiency but also creates a fundamental conflict with the stochastic exploration required by reinforcement learning.

SDE-Based GRPO Methods. Let $s_t = (c, t, x_{t+\Delta t})$ be the state at timestep t, where c represents the generation conditions. GRPO [29], as one of the policy gradient methods [27, 28, 34], directly optimizes the parameters θ of a policy $\pi_{\theta}(x_t|s_t)$, which is the conditional probability distribution defined by the generative model. A reward function

 $R(x_0; c)$, given only at the terminal timestep, defines the supervision reward r. GRPO defines a group-wise normalized advantage function, computed from G rollout samples:

$$A_i = \frac{r_i - \operatorname{mean}(\{r_1, \dots, r_G\})}{\operatorname{std}(\{r_1, \dots, r_G\})}.$$
 (3)

Similar to PPO [28] using clipped policy ratio between old and on-the-fly policies, the GRPO objective is written as

$$\mathcal{J}(\theta) = \mathbb{E}_{s,t,i} \left[\min \left(A_i \rho_t^{(i)}, A_i \lceil \rho_t^{(i)} \rfloor \right) \right] + \beta D_{kl} [\pi_{\theta_{old}} || \pi_{\theta}], \tag{4}$$

where $\rho_t^{(i)} = \frac{\pi_{\theta}(x_t^{(i)}|s_t^{(i)})}{\pi_{\theta_{\text{old}}}(x_t^{(i)}|s_t^{(i)})}$ is the policy ratio and $\lceil \cdot \rfloor$ denotes ratio clipping. It is popular in recent studies to remove the KL-divergence term [14, 41], since the ratio clip with a tiny threshold $(10^{-4} \text{ in DanceGRPO})$ and MixGRPO) strongly ensures the parameters in the trust region.

To introduce stochasticity into the deterministic ODE framework to support policy gradient optimization, SDE-based GRPO methods [17, 41] adopt SDE sampling with the same marginal probability density as the original ODE:

$$x_{t-\Delta t}^{(\text{SDE})} = x_{t-\Delta t}^{(\text{ODE})} - \frac{\sigma_t^2}{2t} \hat{\epsilon}_{\theta}(x_t, t) + \sigma_t \epsilon, \tag{5}$$

where $\hat{\epsilon}_{\theta} = x_t + (1-t)v_{\theta}(x_t,t)$ is the estimated initial noise according to flow matching (Eq. 2). It illustrates the drift term of the SDE. σ_t is a factor controlling the strength of stochasticity, and $\epsilon \sim \mathcal{N}(0,I)$ is independent Gaussian noise. We adopt a formulation that is slightly different from but equivalent to that in previous literature, and we provide a derivation in the Appendix. Under this framework, the policy $\pi_{\theta}(x_t|s_t)$ becomes an isotropic Gaussian distribution of x_t conditioned on $x_{t+\Delta t}$ whose likelihood can be explicitly computed in an exp-MSE form, thus supporting optimization of the GRPO objective.

3.2. SDE-Based GRPO Is Secretly Contrastive Learning

To better understand the optimization mechanism of SDEbased GRPO, we reexamine its optimization dynamics from a distance optimization perspective. This analysis will lay the theoretical foundation for our proposed method.

The policy ratio objective is referred to as the Conservative Policy Iteration (CPI) objective [10, 27–29]. It has been proven to be an estimation of the vanilla policy gradient or REINFORCE objective [34], which is a log-likelihood expectation $\mathbb{E}[A_i\nabla_\theta\log\pi_\theta(x_t^{(i)}\mid s_t^{(i)})].$ The error is bounded by the policy difference $\theta-\theta_{\rm old}$ [10, 27]. The core of this log-policy term in SDE-based GRPO is the negative squared distance. Since the policy ratio is clipped into the trust region [27, 28], we have $\theta\approx\theta_{\rm old}$. Therefore, maximizing the SDE-based GRPO objective is equivalent to mini-

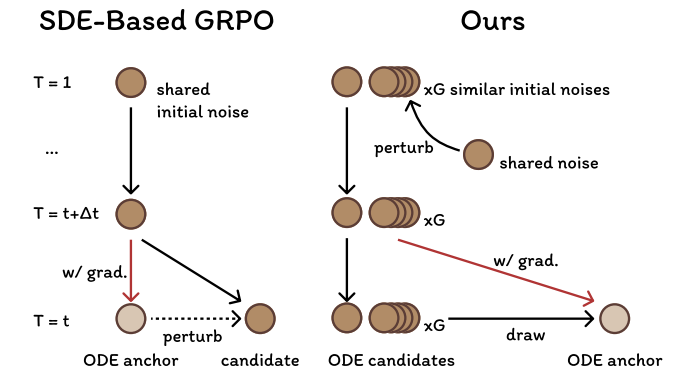


Figure 2. Different from SDE-based GRPO approaches, which explore the sample space with noise perturbation defined by SDE, we directly construct a group of similar initial noises, and conduct deterministic ODE sampling.

mizing an advantage-weighted MSE loss:

$$-\log \pi_{\theta} = \frac{1}{2\sigma_{t+\Delta t}^{2}} \left\| \tilde{x}_{t}^{(\text{ODE})} - x_{t}^{(\text{ODE})} + o_{t}(x_{t+\Delta t}) \right\|_{2}^{2},$$
(6)

where the constant term is omitted, and $\tilde{x}_t^{(\mathrm{ODE})} = x_t^{(\mathrm{ODE})} + \sigma_{t+\Delta t}\epsilon$ is the perturbed ODE sample. The $o_t(x_{t+\Delta t})$ term denotes a drift residual. As the policy θ is constrained to the trust region of θ_{old} [27, 28], this residual term $o(\cdot)$ approaches zero and contributes minimally to the optimization. We present the full derivation in the Appendix.

This form reveals the core optimization mechanism of SDE-based GRPO: advantage-weighted policy gradient updates are equivalent to making the ODE sample approximate nearby stochastically perturbed targets. See Figure 1. This is a distance optimization process. With advantage weighting, high-reward samples (positive A_i) are pulled closer, and low-reward samples (negative A_i) are pushed away, essentially forming a contrastive learning [1, 4, 6, 25] mechanism centered on the one-step ODE trajectory.

3.3. Neighbor GRPO

SDE-based GRPO can be viewed as contrastive learning: ODE anchors are pulled toward high-reward SDE samples and pushed away from low-reward ones. Since candidates act only as reference points and do not backpropagate, we ask: can we eliminate SDEs and optimize a distance objective directly in the ODE neighborhood?

We propose a method following this intuition. Instead of using SDEs to generate stochastic variations for exploration, we create a set of candidate trajectories by perturbing the initial noise of the deterministic ODE solver (Figure 2). Given a base initial noise ϵ^* , we construct G initial conditions:

$$\epsilon^{(i)} = \sqrt{1 - \sigma^2} \epsilon^* + \sigma \delta^{(i)}, \quad i = 1, \dots, G,$$
 (7)

where $\delta^{(i)} \sim \mathcal{N}(0, I)$ and $\sigma \in (0, 1)$ controls the perturbation strength. Evolving these conditions produces a bundle

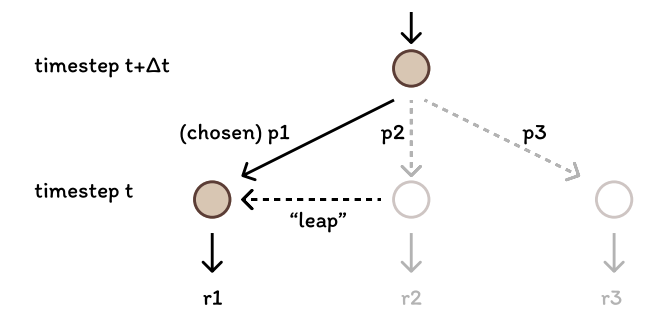


Figure 3. Surrogate leaping policy. The ongoing sampling trajectory virtually leaps to another, following the policy distribution: $p_i = \pi_\theta \left(x_t^{(i)} \mid \{s_t\} \right)$.

of trajectories forming a local solution neighborhood.

To fit GRPO, a stochastic policy $\pi_{\theta}(x_t|s_t)$ among those trajectories is required, but ODE sampling is deterministic. We therefore introduce a training-only *surrogate policy* that enables policy ratios and gradients while keeping inference fully deterministic.

Softmax-Distance Is a Natural Choice. This surrogate should (1) favor candidates closer to the anchor, (2) be tractable for policy gradients, and (3) align with contrastive learning. The softmax distribution over negative squared distances meets these criteria, paralleling soft nearest neighbor [4] and InfoNCE [22]. We define the *surrogate leaping policy* over G candidates in a GRPO batch at timestep t:

$$\pi_{\theta}\left(x_{t}^{(i)} \mid \{s_{t}\}\right) = \frac{\exp\left(-\|x_{t}^{(i)} - x_{t}^{(\theta)}\|_{2}^{2}\right)}{\sum_{k=1}^{G} \exp\left(-\|x_{t}^{(k)} - x_{t}^{(\theta)}\|_{2}^{2}\right)}, \quad (8)$$

where $\{s_t\} = \{s_t^{(1)}, s_t^{(2)}, \dots, s_t^{(G)}\}$ is the group state. The anchor $x_t^{(\theta)}$ is randomly drawn from the candidates $\{x_t\}$, and it contributes gradients to the parameters θ . This distribution typically assigns the highest probability to the nearest candidate, which is often the anchor itself.

Virtual Leaping in the ODE Neighborhood. We interpret π_{θ} as a virtual stochastic process over the ODE neighborhood (Figure 3): at each t, the trajectory may "leap" to a neighbor with probability π_{θ} , most often staying on the anchor. The surrogate policy approximately preserves the ODE marginal (see Appendix for derivation).

This surrogate is an *implicit training tool*, not an inference mechanism. During training it provides policy ratios and gradients that bias the anchor toward high-reward regions; at inference we run standard deterministic ODE sampling without leaping or softmax computation.

Optimization Dynamics. Maximizing its policy gradient via the GRPO objective (Eq. 4) yields a simple geometry: for $A_i > 0$, the gradient decreases the distance $\|x_t^{(i)} - x_t^{(\theta)}\|_2^2$, pulling the anchor toward $x_t^{(i)}$; for $A_i < 0$, it pushes the anchor away. Thus, distance-based contrastive learning is realized within a policy-gradient framework while preserving deterministic ODE inference.

3.4. Practical Implementations

In this section, we introduce three key implementation strategies that significantly enhance the method's practical effectiveness: (1) *symmetric anchor sampling* that exploits the neighborhood structure to reduce the number of backward passes per iteration; (2) a *group-wise quasi-norm advantage reweighting* mechanism that addresses the challenge of reward flattening in later training stages, preventing the model from being trapped in local optima and ensuring continued improvement; (3) usage of *high-order solvers* such as DPM++, enabling faster sampling and better generation quality.

3.4.1. Symmetric Anchor Sampling

Due to the Johnson–Lindenstrauss Lemma [9], the initial noises in a sample group (as formulated in Eq. 7) are almost equidistant. This provides a symmetry of the samples: each one is a "center" for the others. Due to this symmetry, any candidate in the sample group is a potential choice of anchor. This symmetric anchor sampling strategy enables a reduction in the number of required anchors during one GRPO iteration. Concretely, the GRPO objective for a drawn anchor with index k at time t is

$$\sum_{i=1}^{G} \min\left(A_i \, \rho_t^{(i|k)}, \, A_i \left\lceil \rho_t^{(i|k)} \right\rfloor\right), \tag{9}$$

where $\rho_t^{(i|k)}$ is the anchor-conditioned policy ratio:

$$\rho_t^{(i|k)} = \frac{\pi_{\theta}(x_t^{(i)} \mid \{s_t\})}{\pi_{\theta_{\text{old}}}(x_t^{(i)} \mid \{s_t\})} \bigg|_{x_t^{(\theta)} = x_t^{(k)}}.$$
 (10)

In the surrogate leaping policy (Eq. 8), since all candidate samples $x_t^{(i)}$ are generated by the old policy and only the anchor path $x_t^{(\theta)}$ depends on θ , computing this objective and its gradient requires a single forward–backward pass per GRPO batch. Note that existing SDE-based GRPO approaches [14, 41] are typically sample-wise and require G such calculations instead. For commonly used FLUX training with G=12, our method saves up to 12 times of the forward-backward calculations during policy update. This is a strong advantage of our proposed group-wise method.

In practice, because of the symmetry, we sample B anchors per GRPO iteration to estimate a more accurate gradient. Since B < G, this few-anchor speed-up still benefits training by balancing performance and computational cost.

3.4.2. Group-Wise Quasi-Norm Advantage Reweighting

A key challenge in our neighborhood-based optimization arises when the advantage signal flattens after sufficient optimization. The softmax mechanism in our surrogate policy relies on advantage-weighted distances to distinguish high-reward from low-reward candidates. However, when



Figure 4. Effect of quasi-norm reweighting.

all samples in a group yield similar rewards, the standard GRPO normalization (Eq. 3) produces a nearly uniform advantage distribution. Although these advantages are numerically small, they still guide the optimization, leading to weak, over-averaged updates that can cause reward hacking artifacts such as generic average faces in portrait generation (Figure 4a). This issue of flattened rewards is a known challenge in GRPO and related methods [18, 42].

Standard GRPO normalization projects the advantage vector $\mathbf{A}=(A_1,\dots,A_G)$ onto an L_2 -sphere of fixed radius, treating all groups equally regardless of the internal structure of their reward signals. We propose to replace this with a group-wise quasi-normalization based on the L_p -norm with p<2:

$$A_i' = \frac{A_i}{\left(\sum_{k=1}^G |A_k|^p\right)^{1/p}}, \quad p \in (0, 2].$$
 (11)

The insight is that quasi-norms with p < 2 exhibit sparsity-inducing behavior. For a flat advantage vector where all $|A_k|$ are approximately equal, the L_p -norm grows approximately as $G^{1/p}$, which is large when p is small. Dividing by this large norm shrinks the rescaled advantages A_i' , effectively down-weighting the contribution of this uninformative group to the overall gradient. When p=2, the L_2 -norm becomes independent of the sparsity pattern (up to variance), recovering the standard GRPO normalization.

This reweighting mechanism is compatible with existing GRPO clipping schemes and introduces negligible computational overhead. Crucially, it preserves the sign and relative ordering of advantages within each group, maintaining the contrastive learning dynamic while adaptively emphasizing groups that provide clear optimization signals.

3.4.3. Usage of High-Order Solvers

Decoupling full-ODE sampling from the distance-based policy enables us to adopt high-order solvers such as DPM++ [20] to improve both training efficiency and final performance. Concretely, we roll out all trajectories with DPM++ for data collection, while during policy updates we use a one-step DDIM [31] transition from $x_{t+\Delta t}$ to x_t to compute the surrogate policy and the GRPO objective.

Method	Solverold	$NFE_{old} \downarrow$	$\mathbf{NFE}_{ heta}{\downarrow}$	s / Iter.↓	HPSv2.1↑	Pick↑	Img.Rwd.↑	CLIP↑	Unified.↑	Aes.↑
†FLUX.1-dev	N/A	N/A	N/A	N/A	0.310	0.227	1.131	0.389	3.211	6.108
†DanceGRPO	DDIM	25	14	237.86	0.371	0.231	1.306	0.364	3.156	6.552
†MixGRPO	DDIM	25	14	237.71	0.366	0.235	<u>1.604</u>	0.382	3.257	6.623
-Flash*	DPM++	8	4	129.36	0.343	0.228	<u>1.409</u>	0.374	3.148	6.770
NeighborGRPO	DDIM	25	4	141.93	0.359	0.234	1.571	0.385	3.262	6.669
NeighborGRPO	DPM++	16	3	105.85	0.369	0.236	1.643	0.386	3.324	6.633
NeighborGRPO	DPM++	8	1.33	45.08	0.366	0.234	1.640	0.391	3.334	6.621

Table 1. Comparison of human preference scores. <u>Underline</u>: in-domain preference. †: official checkpoints.

4. Experimental Results

We closely follow existing protocols [14, 41] to conduct training and evaluations for a fair comparison. We choose FLUX.1-dev [12] as the base model to evaluate all the algorithms. We adopt the HPDv2 training and test sets, which is an official dataset used by HPSv2 [38]. It includes 103,700 prompts, from which 4800 or 9600 are randomly sampled for training over 300 iterations with a batch size of 16 or 32. The full 3200-sample test set is adopted to evaluate each model. We train each model with the AdamW optimizer for 300 iterations, with a learning rate of 10^{-5} and a batch size of 1 per GPU. For ablation studies, we use 16 GPUs to reduce the cost. For the model performance evaluation and comparison in Table 1, we use 32 GPUs, following existing protocols [14, 41]. In single reward training and ablation studies, we adopt the HPSv2.1 score [38] as the optimization target. Following MixGRPO, we evaluate multireward training with HPSv2.1, Pick Score [11] and ImageReward [40], because this joint training is demonstrated to be effective against reward hacking [14, 41]. We evaluate the models using a multi-dimensional benchmark to cover both in-domain and out-of-domain assessments, consisting of CLIP Score [8], LAION Aesthetic Score [26], and UnifiedReward [37]. We also report the number of function evaluations (NFEs) [19] to assess the training cost.

4.1. Comparison

We select DanceGRPO [41] and MixGRPO [14] as baselines, and compare our Neighbor GRPO with them. They stand for pure SDE-based approaches and SDE-ODE mixed methods, respectively. We also reproduce recently proposed BranchGRPO [15] for reference.

Single Target. See Table 2. When training with HPSv2.1, our approach strikes a balance between training efficiency and final performance, with remarkable performance on both in-domain (HPSv2.1) and out-of-domain evaluations.

As presented in Figure 5, our approach converges faster than the DanceGRPO baseline, reaching an HPSv2.1 score of over 0.35 with only 50 iterations. It also achieves better training stability than MixGRPO in long-term training,

Method	HPSv2.1	CLIP	Unified.	Aes.
DanceGRPO	0.356	0.366	3.114	6.400
MixGRPO	0.371	0.367	3.125	6.365
BranchGRPO	0.379	0.362	3.138	6.571
Ours $p=2$	0.379	0.368	3.132	6.503
Ours $p = 0.8$	0.372	0.371	3.166	6.626

Table 2. Various approaches optimized toward HPSv2.1.

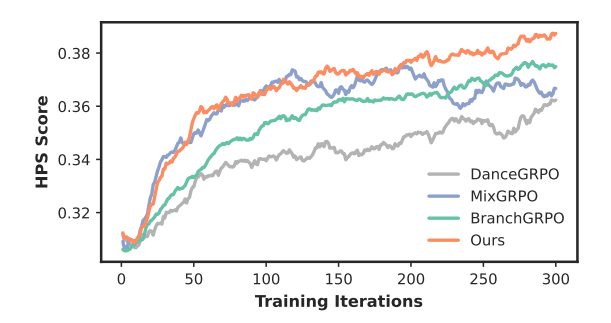


Figure 5. Training curves towards HPSv2.1.

implying a possibility for further scaling up.

Multiple Targets. To achieve the best visual quality, we follow existing protocols to train the model with multiple rewards. See Table 1. We apply the same multi-reward objective as MixGRPO, which adopts HPSv2.1, Pick Score, and Image Reward with equal weights. In 25-step DDIM rollout experiments, our model achieves the highest scores on all out-of-domain evaluations, while remaining on par with the baselines on in-domain evaluations. We believe this high out-of-domain performance is a positive sign, implying robustness against reward hacking and demonstrating the superiority of our approach. In few-step DPM++ solver experiments comparing to MixGRPO-Flash, our approach achieves remarkable performance in most metrics with both 16-step and 8-step rollouts. This proves our model is effective in few-step DPM++ training, demonstrating the superiority of our full-ODE scheme.

Method	NFE _{old}	G	B	K	\mathbf{NFE}_{θ}	s / Iter.
DanceGRPO	25	12	12	14	14.00	237.86
MixGRPO	25	12	12	14	14.00	237.71
-Flash*	$\bar{8}$	12	12	4	4.00	129.36
BranchGRPO	20	16	adapt	4	13.68	249.33
Ours 25-step	25	12	12	4	4.00	141.93
Ours 16-step	16	12	4	9	3.00	105.85
Ours 8-step	8	12	4	4	1.33	45.08

Table 3. Training cost of different methods.

Training Efficiency. We analyze the training efficiency in Table 1, and list more details in Table 3. Thanks to the symmetric anchor sampling strategy, our approach also requires fewer forward/backward calculations during policy update. Given that B is the number of anchors sampled in one GRPO iteration, and G denotes the GRPO group size. Let K denote how many timesteps are updated in a GRPO iteration, usually related to the parameter timestep_fraction. The training cost during policy update is O(BK). Since the baseline methods require a network forward pass for each sample (i.e. B = G), the influence of B on training cost is usually omitted in the literature. To align with previous approaches, we report an effective NFE per sample, calculated as NFE $_{\theta} = \frac{B}{G} \cdot K$. In our experiments, we always use G = 12.

Note that the training time per iteration in Table 3 shows a linear reduction as NFE_{θ} decreases. We emphasize that the policy update occupies the major part during the whole training, because the forward-backward calculation (with even slower gradient checkpoints) is much more costly than forward-only sampling. Our approach is demonstrated to be effective in reducing this part of cost from over 100 to 45 seconds per iteration. For a standard 300-iteration training, it takes about 4 hours on 32 NVIDIA H800 GPUs, which makes the GRPO training of flow models more practical.

Qualitative Results. We present samples in Figure 6 and the Appendix. The images are generated with models trained with our approach (Ours with DPM++ solver and NFE_{old} = 8 in Table 1) and the released baseline methods. Compared to baselines, our model better understands the user prompt and generates high-quality results without reward hacking artifacts like grid patterns and imbalanced color distribution. This visualization demonstrates the quantitative results in Table 1: our approach achieves better human preference alignment without hacking the indomain reward models.

Human Evaluation. RLHF approaches are known to suffer from the reward hacking issue [41]. Therefore, to further demonstrate our approach, we conduct a user study to compare the win rates against the baselines. We ask 46 users covering various professional backgrounds to choose the



A low poly lemon in high quality rendering



A hamster resembling a horse



Peter Griffin taking a selfie in a park on an iPhone 12 Pro.



A whale is reading a book about avoiding Japanese spears in an underwater library.

Figure 6. Visualization of different approaches.

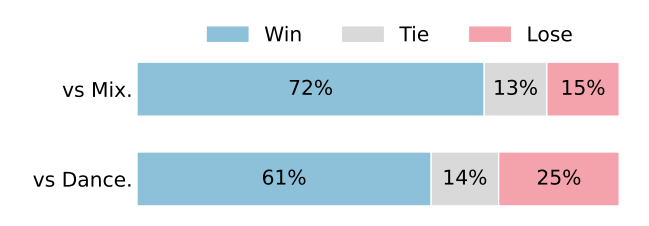


Figure 7. Human evaluation comparing our method with baselines.

preferred image from each pair generated from the same HPDv2 prompt using different models. As shown in Figure 7, our approach achieves higher human preference ratings (72% and 61%) than the baselines on the evaluated text-to-image generation tasks.



Figure 8. Rollout groups after 300-iteration training. $\sigma = 0.3$.

4.2. Ablation Study

We conduct a series of ablation studies to validate the effectiveness and parameter choices of the core components of Neighbor GRPO: the randomness strength σ of ODE neighborhood sampling, the batch size B of symmetric anchor sampling strategy, and the quasi-norm reweighting parameter p. We set $(\sigma,B,p)=(0.5,4,2)$ as the initial baseline for ablation and study around this default setup.

Impact of ODE Neighborhood Sampling. To verify the necessity of our proposed neighborhood sampling strategy, we analyze the impact of the initial noise perturbation strength σ . As shown in Table 4, we experiment with different values for σ in $\{0.1, 0.3, 0.5, 1.0\}$. We expect to find an optimal range; a value that is too small would create a neighborhood that is too tight for effective exploration, while a value that is too large would make the contrastive learning task too difficult and raise the risk of reward hacking, as the samples would no longer be considered neighbors. As the results show in Table 4, a larger σ leads to better in-domain performance but may result in worse out-of-domain performance. We find that $\sigma=0.3$ is a suitable choice. Figure 8 shows the sample diversity after sufficient training.

Symmetric Anchor Sampling. We investigate the influence of the number of anchors for each GRPO iteration. Table 5 presents the results. With only B=2 anchors sampled, the HPSv2.1 score achieves over 0.37, which is a competitive performance. Note that in this situation, the policy-update process is 6 times faster. With a larger B=4 setup, all performance metrics improved. We find this to be a good balance between performance and training cost.

Group-Wise Quasi-Norm Reweighting. We validate our proposed Group-wise Quasi-Norm Reweighting by comparing it against the standard advantage normalization used in GRPO. See Table 6. We experiment with different values of p in our L_p -norm, such as $\{0.5, 0.8, 1, 2\}$. The case where p=2 recovers the performance of standard group normalization. The results confirm that a value of p=0.8 is more effective against reward hacking, yielding the best out-of-domain scores. When adopting a smaller p value, the

σ	HPSv2.1	CLIP	Unified.	Aes.
1.0	0.364	0.359	3.046	6.362
0.5	0.379	0.368	3.132	6.503
0.3	0.375	0.363	3.141	6.639
0.1	0.357	0.364	3.122	6.295

Table 4. Performance with various p normalization.

В	HPSv2.1	CLIP	Unified.	Aes.
2	0.370	0.363	3.081	6.319
4	0.379	0.368	3.132	6.503
8	0.374	0.373	3.187	6.403
12	0.377	0.370	3.185	6.328

Table 5. Performance of various number of sampled anchors.

\overline{p}	HPSv2.1	CLIP	Unified.	Aes.
2 (GRPO)	0.379	0.368	3.132	6.503
1	0.377	0.356	3.126	6.508
0.8	0.372	0.371	3.166	6.626
0.5	0.372	0.354	3.104	6.548

Table 6. Performance with various p normalization.

model lacks exploration, as indicated by a decrease across all scores. The quantitative results demonstrate that the choice of a non-Euclidean norm is a critical factor.

5. Conclusion

In this paper, we introduced Neighbor GRPO, a novel RLHF paradigm for aligning flow matching models that completely bypasses the need for SDE conversion. Our core insight is to reinterpret the optimization dynamics of existing SDE-based GRPO methods as a form of distance-based contrastive learning. Based on this, we integrated a surrogate leaping policy into the GRPO framework, which provides both the necessary stochastic abstraction and contrastive learning dynamics. Furthermore, we assess practical implementations.

Our extensive experiments demonstrated that Neighbor GRPO significantly outperforms SDE-based counterparts. It fully preserves the advantages of deterministic ODE sampling, including compatibility with high-order solvers. The method achieves faster convergence and superior generation quality, highlighting the effectiveness of its more direct credit assignment mechanism.

For future work, we plan to extend this approach to video generation. The efficiency of Neighbor GRPO makes it particularly suitable for the high computational demands of video synthesis. We will also explore its application in scenarios where rewards are scarce or noisy, as the neighborhood contrastive learning may offer greater robustness.

Algorithm 1 Neighbor GRPO

```
Require: prompts C, parameters \theta; group size G; anchors
     per batch B; number of rollout steps T; number of train
     steps K; time schedule \mathcal{T} = \{t_1, t_2, \dots, t_T\}
Ensure: t_T = 1, t_1 = 0
     for iteration m = 1 to M do
             \pi_{\theta_{\text{old}}} \leftarrow \pi_{\theta}
             Sample prompt c \in C
            Draw shared initial noise \epsilon^* \sim \mathcal{N}(0, I)
            for i = 1 to G do
                    Draw \delta^{(i)} \sim \mathcal{N}(0, I)
                    x_1^{(i)} \leftarrow \sqrt{1 - \sigma^2} \epsilon^* + \sigma \delta^{(i)}
                                                                                          ⊳ Perturb noise.
                    for k = T to 1 do
x_{t_{k-1}}^{(i)} \leftarrow \text{RolloutSolver.step}(x_{t_k}^{(i)}, c; \theta_{\text{old}})
                    end for
            end for
             Compute advantages \{A_i\}
             Sample B anchor indices S \subset \{1, \dots, G\}
             Sample K steps \mathcal{K} \subset \{1, 2, \dots, T-1\}
            for j \in S do
                  \begin{aligned} &\text{for } k \in \mathcal{K} \text{ do} \\ &x_{t_{k+1}}^{(\theta)} \leftarrow x_{t_{k+1}}^{(j)} \\ &x_{t_k}^{(\theta)} \leftarrow \text{TrainSolver.step} \big( x_{t_{k+1}}^{(\theta)}, c; \theta \big) \\ &\text{for } i = 1 \text{ to } G \text{ do} \\ &x_{\theta}^{(i)} \leftarrow \text{softmax}_i \big( -\| x_{t_k}^{(i)} - x_{t_k}^{(\theta)} \|_2^2 \big) \\ &x_{\theta_{\text{old}}}^{(i)} \leftarrow \text{softmax}_i \big( -\| x_{t_k}^{(i)} - x_{t_k}^{(j)} \|_2^2 \big) \\ &\rho^{(i|j)} \leftarrow \pi_{\theta}^{(i)} / \pi_{\theta_{\text{old}}}^{(i)} \end{aligned}
                            end for
                            Compute J = J(A, \rho; \theta)
                            Accumulate gradients \nabla_{\theta} J
                    Update \theta using accumulated gradients
            end for
     end for
```

Appendix

I. Algorithm

We provide the pseudo-code for Neighbor GRPO in Algorithm 1. We suggest adopting a more efficient solver, such as DPM-Solver++, with fewer sampling timesteps T for the RolloutSolver to accelerate training. Compared with SDE-based GRPO methods, which call TrainSolver $G \times K$ times in each GRPO iteration, our approach requires $B \times K$ calls to TrainSolver. Note that we usually have B < G, which allows us to further reduce the training cost with Neighbor GRPO.

II. Derivation of the SDE Formulation

For a Rectified Flow model, the forward process from data x_0 to noise ϵ is $x_t = (1-t)x_0 + t\epsilon$. The reverse process follows the ODE $\frac{dx_t}{dt} = v_\theta(x_t,t)$, where $v_\theta(x_t,t) \approx \epsilon - x_0$.

To introduce stochasticity, we construct an equivalent SDE that shares the same marginal probability density $p_t(x)$ for all $t \in [0, 1]$. A common choice is:

$$dx_t = \left[v_\theta(x_t, t) + \frac{\eta_t^2}{2t}\hat{\epsilon}_\theta(x_t, t)\right]dt + \eta_t dw_t, \qquad (12)$$

where dw_t is a standard Wiener process, η_t controls the noise intensity, and $\hat{\epsilon}_{\theta}(x_t,t) = x_t + (1-t)v_{\theta}(x_t,t)$ is the estimated initial noise.

For numerical simulation, we discretize the reverse SDE. With a backward step $\Delta t>0$, the update rule is:

$$x_{t-\Delta t} = x_t - \left[v_{\theta}(x_t, t) + \frac{\eta_t^2}{2t} \hat{\epsilon}_{\theta}(x_t, t) \right] \Delta t + \eta_t \sqrt{\Delta t} \epsilon,$$
(13)

where $\epsilon \sim \mathcal{N}(0,I)$. Let's define the single-step ODE update as $x_{t-\Delta t}^{(\text{ODE})} = x_t - v_{\theta}(x_t,t)\Delta t$. Let $\sigma_t^2 = \eta_t^2 \Delta t$. The SDE update can be rewritten as:

$$x_{t-\Delta t}^{(\text{SDE})} = x_t - v_{\theta}(x_t, t)\Delta t - \frac{\sigma_t^2}{2t\Delta t}\hat{\epsilon}_{\theta}(x_t, t)\Delta t + \sigma_t \epsilon$$
(14)

$$= x_{t-\Delta t}^{(\text{ODE})} - \frac{\sigma_t^2}{2t} \hat{\epsilon}_{\theta}(x_t, t) + \sigma_t \epsilon.$$
 (15)

This discretized update defines a Gaussian policy $\pi_{\theta}(x_{t-\Delta t}|x_{t},c) = \mathcal{N}(\mu_{\theta},\sigma_{t}^{2}I)$, where the mean is $\mu_{\theta}(x_{t},t) = x_{t-\Delta t}^{(\mathrm{ODE})} - \frac{\sigma_{t}^{2}}{2t}\hat{\epsilon}_{\theta}(x_{t},t)$. The negative log-likelihood of this policy is:

$$-\log \pi_{\theta}(x_{t-\Delta t} \mid x_{t}, c) = \frac{1}{2\sigma_{t}^{2}} \|x_{t-\Delta t} - \mu_{\theta}(x_{t}, t)\|_{2}^{2} + \text{const.}$$
(16)

This provides the basis for the distance-based contrastive learning interpretation of SDE-based GRPO.

III. Derivation of the Drift Residual

The objective of GRPO is to maximize the expected log-likelihood of samples from the old policy $\pi_{\theta_{\text{old}}}$ under the new policy π_{θ} . This is equivalent to minimizing the negative log-likelihood:

$$\mathcal{L}(\theta) = \mathbb{E}_{x_{t-\Delta t} \sim \pi_{\theta_{\text{old}}}} \left[-\log \pi_{\theta}(x_{t-\Delta t}) \right]. \tag{17}$$

From the SDE formulation in the previous section, the policy π_{θ} is an isotropic Gaussian distribution $\pi_{\theta}(x_{t-\Delta t}|x_{t}) = \mathcal{N}(\mu_{\theta}, \sigma_{t}^{2}I)$. The mean μ_{θ} and a sample

from the old policy $x_{t-\Delta t}^{(\mathrm{SDE},\mathrm{old})}$ are given by:

$$\mu_{\theta} = x_{t-\Delta t}^{(\text{ODE},\theta)} - \frac{\sigma_t^2}{2t} \hat{\epsilon}_{\theta}(x_t, t), \tag{18}$$

$$x_{t-\Delta t}^{(\text{SDE,old})} = x_{t-\Delta t}^{(\text{ODE,old})} - \frac{\sigma_t^2}{2t} \hat{\epsilon}_{\theta_{\text{old}}}(x_t, t) + \sigma_t \epsilon, \quad (19)$$

where $\epsilon \sim \mathcal{N}(0, I)$, and the superscripts denote the policy parameters used for the ODE step and noise prediction.

The negative log-likelihood term, omitting constants, is a mean squared error (MSE):

$$-\log \pi_{\theta}(x_{t-\Delta t}^{(\text{SDE,old})}) = \frac{1}{2\sigma_t^2} \left\| x_{t-\Delta t}^{(\text{SDE,old})} - \mu_{\theta} \right\|_2^2. \quad (20)$$

Substituting the expressions for the mean and the sample, we get the term inside the norm:

$$x_{t-\Delta t}^{(\text{SDE,old})} - \mu_{\theta}$$

$$= \left(x_{t-\Delta t}^{(\text{ODE,old})} - \frac{\sigma_{t}^{2}}{2t} \hat{\epsilon}_{\theta_{\text{old}}} + \sigma_{t} \epsilon \right) - \left(x_{t-\Delta t}^{(\text{ODE},\theta)} - \frac{\sigma_{t}^{2}}{2t} \hat{\epsilon}_{\theta} \right)$$
(21)
$$\left((\text{ODE,old}) + (\text{ODE},\theta) + (\sigma_{t}^{2} + \sigma_{t}^{2} + \sigma_{t}^{2}) \right)$$

$$= \left(x_{t-\Delta t}^{(\text{ODE,old})} + \sigma_t \epsilon\right) - x_{t-\Delta t}^{(\text{ODE},\theta)} - \left(\frac{\sigma_t^2}{2t} \hat{\epsilon}_{\theta_{\text{old}}} - \frac{\sigma_t^2}{2t} \hat{\epsilon}_{\theta}\right).$$
(22)

The main paper presents this MSE term in a simplified form:

$$\frac{1}{2\sigma_t^2} \left\| \tilde{x}_{t-\Delta t}^{(\text{ODE})} - x_{t-\Delta t}^{(\text{ODE})} + o_{t-\Delta t}(x_t) \right\|_2^2, \quad (23)$$

where $\tilde{x}_{t-\Delta t}^{(\mathrm{ODE})} = x_{t-\Delta t}^{(\mathrm{ODE},\mathrm{old})} + \sigma_t \epsilon$ is the perturbed ODE sample from the old policy, and $x_{t-\Delta t}^{(\mathrm{ODE})}$ represents the ODE step from the new policy.

By comparing the two forms, we can identify the drift residual term $o_{t-\Delta t}(x_t)$:

$$o_{t-\Delta t}(x_t) = \frac{\sigma_t^2}{2t} \hat{\epsilon}_{\theta}(x_t, t) - \frac{\sigma_t^2}{2t} \hat{\epsilon}_{\theta_{\text{old}}}(x_t, t).$$
 (24)

This term represents the drift correction between the old and new policies. As the policy update is constrained within a trust region, $\theta \approx \theta_{\rm old}$, and this residual term approaches zero.

IV. Marginal Distribution Preservation

Consider the standard flow matching framework with marginal distribution $p_{\theta}(x_t)$ at timestep $t \in [0,1]$, induced by the deterministic ODE flow $\Phi_{1 \to t}(\cdot; \theta)$ starting from initial noise x_1 :

$$p_{\theta}(x_t) = \mathbb{E}_{x_1 \sim \mathcal{N}(0:I)} \left[\delta(x_t - \Phi_{1 \to t}(x_1; \theta)) \right], \tag{25}$$

where $\delta(\cdot)$ is the Dirac delta function. We define a leaping probability $\pi(x_t|x_t') = \mathcal{N}(x_t|x_t',\sigma_\pi I)$, denoting the probability that any reachable latent sample $x_t' = \Phi_{1 \to t}(x_1';\theta)$

(derived from an initial noise x'_1) leaps to x_t . Following this distribution, the marginal distribution of x_t leaped from any x'_t is

$$\pi(x_t) = \int p_{\theta}(x_t')\pi(x_t|x_t')dx_t'. \tag{26}$$

Given a sufficiently small σ_{π} (or as $\sigma_{\pi} \to 0$), the support of $\pi(x_t|x_t')$ collapses to a single point where $x_t'=x_t$. Consequently, $\pi(x_t) \to p_{\theta}(x_t)$.

Now consider a Monte-Carlo approximation of $\pi(x_t)$:

$$\hat{\pi}(x_t) = \frac{1}{G} \sum_{i=1}^{G} \pi(x_t | x_t^{(i)}), \quad x_t^{(i)} \sim p_{\theta}(x_t).$$
 (27)

Let $\hat{\pi}(x_t^{(i)}) = \frac{1}{G}$. We have:

$$\hat{\pi}(x_t^{(i)}|x_t) = \frac{\hat{\pi}(x_t^{(i)})\hat{\pi}(x_t \mid x_t^{(i)})}{\hat{\pi}(x_t)}$$
(28)

$$= \frac{\pi(x_t|x_t^{(i)})}{\sum_{j=1}^G \pi(x_t|x_t^{(j)})}$$
(29)

$$= \frac{\exp(-\|x_t - x_t^{(i)}\|_2^2 / 2\sigma_\pi^2)}{\sum_j \exp(-\|x_t - x_t^{(j)}\|_2^2 / 2\sigma_\pi^2)}.$$
 (30)

This formulation results in a softmax distribution with a temperature of $2\sigma_\pi^2$. In practice, we omit this temperature parameter because the Euclidean distance $\|x_t - x_t^{(i)}\|_2^2$ is empirically large enough when $i \neq j$. Replacing x_t with $x_t^{(\theta)}$ yields the surrogate leaping policy presented in the main paper. Maximizing this posterior probability $\hat{\pi}(x_t^{(i)}|x_t^{(\theta)})$ encourages the generated sample to align closely with the support of the empirical marginal distribution defined by $\{x_t^{(i)}\}_{i=1}^G$. This serves as a tractable surrogate objective for marginal distribution preservation.

V. More Qualitative Results

We present more visualization results comparing different methods in Figure 9.

References

- [1] Sumit Chopra, Raia Hadsell, and Yann LeCun. Learning a similarity metric discriminatively, with application to face verification. In 2005 IEEE computer society conference on computer vision and pattern recognition (CVPR'05), pages 539–546. IEEE, 2005. 2, 4
- [2] Paul F Christiano, Jan Leike, Tom Brown, Miljan Martic, Shane Legg, and Dario Amodei. Deep reinforcement learning from human preferences. *Advances in neural information* processing systems, 30, 2017. 1
- [3] Yihe Deng and Paul Mineiro. Flow-dpo: Improving llm mathematical reasoning through online multi-agent learning. arXiv preprint arXiv:2410.22304, 2024. 1







Two skunks - one small and dark blue with yellow eyes and a larger albino one with red eyes.







Anime-style vector illustration of a cloudy sky with a unique perspective.











The image shows a pirate holding up a beer in celebration.







The image is of a massive cave interior filled with glowing stalactites and stalagmites.







A portrait of a woman with a paper bag over her head.







A snowy lake in Sweden captured in a vibrant, cinematic style with intense detail and raytracing technology showcased on Artstation.







Realism tattoo design sketch of a pirate ship.







A blond person wearing a suit, medical gloves and a skull face mask is shown in a frontal portrait by Kim Kyoung Hwan.







A cat laying on the floor of a kitchen.







A kitchen counter top with a white bowl sitting next to another white bowl.

Figure 9. Visualization of different approaches (DanceGRPO - MixGRPO - NeighborGRPO).

- [4] Nicholas Frosst, Nicolas Papernot, and Geoffrey Hinton. Analyzing and improving representations with the soft nearest neighbor loss. In International conference on machine learning, pages 2012-2020. PMLR, 2019. 2, 4
- [5] Daya Guo, Dejian Yang, Haowei Zhang, Junxiao Song,
- Ruoyu Zhang, Runxin Xu, Qihao Zhu, Shirong Ma, Peiyi Wang, Xiao Bi, et al. Deepseek-r1: Incentivizing reasoning capability in llms via reinforcement learning. arXiv preprint arXiv:2501.12948, 2025. 1
- [6] Kaiming He, Haoqi Fan, Yuxin Wu, Saining Xie, and Ross

- Girshick. Momentum contrast for unsupervised visual representation learning. In *Proceedings of the IEEE/CVF conference on computer vision and pattern recognition*, pages 9729–9738, 2020. 2, 4
- [7] Jonathan Ho, Ajay Jain, and Pieter Abbeel. Denoising diffusion probabilistic models. *Advances in neural information processing systems*, 33:6840–6851, 2020. 1
- [8] Gabriel Ilharco, Mitchell Wortsman, Ross Wightman, Cade Gordon, Nicholas Carlini, Rohan Taori, Achal Dave, Vaishaal Shankar, Hongseok Namkoong, John Miller, Hannaneh Hajishirzi, Ali Farhadi, and Ludwig Schmidt. Openclip, 2021. If you use this software, please cite it as below.
- [9] William B Johnson, Joram Lindenstrauss, et al. Extensions of lipschitz mappings into a hilbert space. *Contemporary mathematics*, 26(189-206):1, 1984.
- [10] Sham Kakade and John Langford. Approximately optimal approximate reinforcement learning. In *Proceedings of the nineteenth international conference on machine learning*, pages 267–274, 2002. 3
- [11] Yuval Kirstain, Adam Polyak, Uriel Singer, Shahbuland Matiana, Joe Penna, and Omer Levy. Pick-a-pic: An open dataset of user preferences for text-to-image generation. Advances in neural information processing systems, 36:36652–36663, 2023. 6
- [12] Black Forest Labs, Stephen Batifol, Andreas Blattmann, Frederic Boesel, Saksham Consul, Cyril Diagne, Tim Dockhorn, Jack English, Zion English, Patrick Esser, Sumith Kulal, Kyle Lacey, Yam Levi, Cheng Li, Dominik Lorenz, Jonas Müller, Dustin Podell, Robin Rombach, Harry Saini, Axel Sauer, and Luke Smith. Flux.1 kontext: Flow matching for in-context image generation and editing in latent space, 2025. 1, 6
- [13] Nathan Lambert, Jacob Morrison, Valentina Pyatkin, Shengyi Huang, Hamish Ivison, Faeze Brahman, Lester James V Miranda, Alisa Liu, Nouha Dziri, Shane Lyu, et al. Tulu 3: Pushing frontiers in open language model posttraining. arXiv preprint arXiv:2411.15124, 2024. 1
- [14] Junzhe Li, Yutao Cui, Tao Huang, Yinping Ma, Chun Fan, Miles Yang, and Zhao Zhong. Mixgrpo: Unlocking flow-based grpo efficiency with mixed ode-sde. *arXiv preprint* arXiv:2507.21802, 2025. 1, 2, 3, 5, 6
- [15] Yuming Li, Yikai Wang, Yuying Zhu, Zhongyu Zhao, Ming Lu, Qi She, and Shanghang Zhang. Branchgrpo: Stable and efficient grpo with structured branching in diffusion models. arXiv preprint arXiv:2509.06040, 2025. 1, 2, 3, 6
- [16] Yaron Lipman, Ricky TQ Chen, Heli Ben-Hamu, Maximilian Nickel, and Matt Le. Flow matching for generative modeling. arXiv preprint arXiv:2210.02747, 2022. 1, 3
- [17] Jie Liu, Gongye Liu, Jiajun Liang, Yangguang Li, Jiaheng Liu, Xintao Wang, Pengfei Wan, Di Zhang, and Wanli Ouyang. Flow-grpo: Training flow matching models via online rl. arXiv preprint arXiv:2505.05470, 2025. 1, 2, 3
- [18] Zichen Liu, Changyu Chen, Wenjun Li, Penghui Qi, Tianyu Pang, Chao Du, Wee Sun Lee, and Min Lin. Understanding r1-zero-like training: A critical perspective. *arXiv preprint arXiv:2503.20783*, 2025. 5

- [19] Cheng Lu, Yuhao Zhou, Fan Bao, Jianfei Chen, Chongxuan Li, and Jun Zhu. Dpm-solver: A fast ode solver for diffusion probabilistic model sampling in around 10 steps. Advances in neural information processing systems, 35:5775– 5787, 2022. 6
- [20] Cheng Lu, Yuhao Zhou, Fan Bao, Jianfei Chen, Chongxuan Li, and Jun Zhu. Dpm-solver++: Fast solver for guided sampling of diffusion probabilistic models. *Machine Intelligence Research*, pages 1–22, 2025. 2, 5
- [21] Bingqi Ma, ZHUOFAN ZONG, Guanglu Song, Hongsheng Li, and Yu Liu. Exploring the role of large language models in prompt encoding for diffusion models. Advances in Neural Information Processing Systems, 37:118428–118455, 2024. 1
- [22] Aaron van den Oord, Yazhe Li, and Oriol Vinyals. Representation learning with contrastive predictive coding. arXiv preprint arXiv:1807.03748, 2018. 4
- [23] Long Ouyang, Jeffrey Wu, Xu Jiang, Diogo Almeida, Carroll Wainwright, Pamela Mishkin, Chong Zhang, Sandhini Agarwal, Katarina Slama, Alex Ray, et al. Training language models to follow instructions with human feedback. Advances in neural information processing systems, 35:27730–27744, 2022. 1
- [24] Robin Rombach, Andreas Blattmann, Dominik Lorenz, Patrick Esser, and Björn Ommer. High-resolution image synthesis with latent diffusion models. In *Proceedings of* the IEEE/CVF conference on computer vision and pattern recognition, pages 10684–10695, 2022. 1
- [25] Florian Schroff, Dmitry Kalenichenko, and James Philbin. Facenet: A unified embedding for face recognition and clustering. In *Proceedings of the IEEE conference on computer vision and pattern recognition*, pages 815–823, 2015. 2, 4
- [26] Christoph Schuhmann, Romain Beaumont, Richard Vencu, Cade Gordon, Ross Wightman, Mehdi Cherti, Theo Coombes, Aarush Katta, Clayton Mullis, Mitchell Wortsman, et al. Laion-5b: An open large-scale dataset for training next generation image-text models. Advances in neural information processing systems, 35:25278–25294, 2022. 6
- [27] John Schulman, Sergey Levine, Pieter Abbeel, Michael Jordan, and Philipp Moritz. Trust region policy optimization. In *International conference on machine learning*, pages 1889–1897. PMLR, 2015. 3, 4
- [28] John Schulman, Filip Wolski, Prafulla Dhariwal, Alec Radford, and Oleg Klimov. Proximal policy optimization algorithms. *arXiv preprint arXiv:1707.06347*, 2017. 3, 4
- [29] Zhihong Shao, Peiyi Wang, Qihao Zhu, Runxin Xu, Junxiao Song, Xiao Bi, Haowei Zhang, Mingchuan Zhang, YK Li, Yang Wu, et al. Deepseekmath: Pushing the limits of mathematical reasoning in open language models. *arXiv preprint arXiv:2402.03300*, 2024. 1, 2, 3
- [30] Dazhong Shen, Guanglu Song, Yi Zhang, Bingqi Ma, Lujundong Li, Dongzhi Jiang, Zhuofan Zong, and Yu Liu. Adt: Tuning diffusion models with adversarial supervision. *arXiv* preprint arXiv:2504.11423, 2025. 1
- [31] Jiaming Song, Chenlin Meng, and Stefano Ermon. Denoising diffusion implicit models. arXiv preprint arXiv:2010.02502, 2020. 5

- [32] Nisan Stiennon, Long Ouyang, Jeffrey Wu, Daniel Ziegler, Ryan Lowe, Chelsea Voss, Alec Radford, Dario Amodei, and Paul F Christiano. Learning to summarize with human feedback. Advances in neural information processing systems, 33:3008–3021, 2020. 1
- [33] Hongzu Su, Lichao Meng, Lei Zhu, Ke Lu, and Jingjing Li. Ddpo: Direct dual propensity optimization for post-click conversion rate estimation. In Proceedings of the 47th International ACM SIGIR Conference on Research and Development in Information Retrieval, pages 1179–1188, 2024. 1
- [34] Richard S Sutton, David McAllester, Satinder Singh, and Yishay Mansour. Policy gradient methods for reinforcement learning with function approximation. *Advances in neural information processing systems*, 12, 1999. 3
- [35] Bram Wallace, Meihua Dang, Rafael Rafailov, Linqi Zhou, Aaron Lou, Senthil Purushwalkam, Stefano Ermon, Caiming Xiong, Shafiq Joty, and Nikhil Naik. Diffusion model alignment using direct preference optimization. In Proceedings of the IEEE/CVF Conference on Computer Vision and Pattern Recognition, pages 8228–8238, 2024. 1
- [36] Yibin Wang, Zhimin Li, Yuhang Zang, Yujie Zhou, Jiazi Bu, Chunyu Wang, Qinglin Lu, Cheng Jin, and Jiaqi Wang. Pref-grpo: Pairwise preference reward-based grpo for stable text-to-image reinforcement learning. arXiv preprint arXiv:2508.20751, 2025. 1
- [37] Yibin Wang, Yuhang Zang, Hao Li, Cheng Jin, and Jiaqi Wang. Unified reward model for multimodal understanding and generation. arXiv preprint arXiv:2503.05236, 2025. 6
- [38] Xiaoshi Wu, Yiming Hao, Keqiang Sun, Yixiong Chen, Feng Zhu, Rui Zhao, and Hongsheng Li. Human preference score v2: A solid benchmark for evaluating human preferences of text-to-image synthesis. arXiv preprint arXiv:2306.09341, 2023. 6
- [39] Xiaoshi Wu, Yiming Hao, Manyuan Zhang, Keqiang Sun, Zhaoyang Huang, Guanglu Song, Yu Liu, and Hongsheng Li. Deep reward supervisions for tuning text-to-image diffusion models. In *European Conference on Computer Vision*, pages 108–124. Springer, 2024. 1
- [40] Jiazheng Xu, Xiao Liu, Yuchen Wu, Yuxuan Tong, Qinkai Li, Ming Ding, Jie Tang, and Yuxiao Dong. Imagereward: Learning and evaluating human preferences for texto-image generation. Advances in Neural Information Processing Systems, 36:15903–15935, 2023. 1, 6
- [41] Zeyue Xue, Jie Wu, Yu Gao, Fangyuan Kong, Lingting Zhu, Mengzhao Chen, Zhiheng Liu, Wei Liu, Qiushan Guo, Weilin Huang, et al. Dancegrpo: Unleashing grpo on visual generation. *arXiv preprint arXiv:2505.07818*, 2025. 1, 2, 3, 5, 6, 7
- [42] Qiying Yu, Zheng Zhang, Ruofei Zhu, Yufeng Yuan, Xiaochen Zuo, Yu Yue, Weinan Dai, Tiantian Fan, Gaohong Liu, Lingjun Liu, et al. Dapo: An open-source Ilm reinforcement learning system at scale. *arXiv preprint arXiv:2503.14476*, 2025. 5
- [43] Zhuofan Zong, Dongzhi Jiang, Bingqi Ma, Guanglu Song, Hao Shao, Dazhong Shen, Yu Liu, and Hongsheng Li. Easyref: Omni-generalized group image reference for diffusion models via multimodal llm. In Forty-second International Conference on Machine Learning, 2024. 1